

Unsteady Aerodynamics of Airfoils Encountering Traveling Gusts and Vortices

J. Gordon Leishman*

University of Maryland, College Park, Maryland 20742

By means of the reverse flow theorems, results are obtained for the unsteady lift and pitching moment on two-dimensional airfoils penetrating sharp-edged traveling gusts. Both downstream and upstream traveling gusts are considered. For the incompressible case, exact results are given and are generalized numerically for any gust field by means of Duhamel superposition. Results are then given for the airloads and acoustics generated by a two-dimensional airfoil encountering a vortex convecting at different gust speed ratios. Numerical results for the traveling sharp-edged gust problem are also derived for subsonic flows by means of exact linear theory. Further results for the subsonic case are computed by means of an Euler finite difference method. It is found that the gust speed ratio has substantial effects on the unsteady airloads and will be an important parameter to represent in helicopter rotor aeroacoustic problems.

Nomenclature

A_i	= coefficients of indicial function
a	= sonic velocity, ms^{-1}
b_i	= exponents of indicial function
C_l	= lift coefficient
C_{l_α}	= lift curve slope, rad^{-1}
C_m	= moment coefficient about quarter-chord
$C_{m_{le}}$	= moment coefficient about leading edge
c	= chord, m
G_i	= coefficients of gust function
g_i	= exponents of gust function
M	= freestream Mach number
q	= nondimensional pitch rate, $\alpha c/V$
R	= rotor radius, m
r	= radial distance from vortex center, m
\bar{r}	= nondimensional distance from hub, y_{ref}/R
r_c	= vortex core radius, m
s	= distance in semichords, $2Vt/c$
t	= time, s
\hat{t}	= time, $t/2M$, s
V	= airfoil velocity relative to flow, ms^{-1}
V_g	= gust convection velocity, ms^{-1}
V_∞	= freestream velocity, ms^{-1}
w	= gust velocity induced normal to airfoil, ms^{-1}
x_v, y_v	= position of vortex, m
x, y	= airfoil coordinate system, measured from leading edge, m
y_{ref}	= distance from rotational axis, m
Z_i	= aerodynamic deficiency functions
α	= angle of attack, rad
α_e	= effective angle of attack, rad
β	= Glauert factor, $\sqrt{1 - M^2}$
Γ	= vortex strength (circulation), m^2s^{-1}
Δ	= incremental quantity
ΔC_p	= differential pressure coefficient
$\delta(t)$	= Dirac delta function
ζ	= nondimensional chord (measured from leading edge), x/c
θ	= angular coordinate, $\cos^{-1}(1 - 2\zeta)$, rad

λ	= gust speed ratio, $V/(V + V_g)$
μ	= advance ratio, $V_\infty/\Omega R$
σ	= dummy variable of integration
ϕ_w	= Wagner indicial response function
ψ	= blade azimuth angle, rad
ψ_K	= Küssner function
Ω	= rotor rotational velocity, rads^{-1}

Superscripts

c	= circulatory part
nc	= noncirculatory part
qs	= quasisteady part

Introduction

THE accurate prediction of the airloads induced on helicopter rotor blades encountering tip vortices generated by other blades is key to predicting the rotor aeroelastic response and rotor acoustics. The rapid changes in angle of attack resulting from the intense velocity gradients generated by blade tip vortices have been identified as significant sources of unsteady aerodynamic loading^{1,2} and a major contributor to rotor noise.^{3,4} Extensive research into the blade vortex interaction (BVI) phenomenon has provided a good amount of fundamental knowledge and has led to an increased appreciation of the difficulties in its prediction.⁵⁻⁹

Comprehensive helicopter rotor analyses contain sophisticated structural dynamics as well as blade unsteady aerodynamics and vortex wake models.^{10,11} These interdependent models must be solved in a fully coupled sense, which places stringent computational demands on the allowable level of unsteady aerodynamic modeling. Although a wide variety of aerodynamic and acoustic models exist, it has not yet proven possible to model the aeroacoustics at the fidelity necessary for acceptable predictions or with reasonable computing costs.¹¹

A particularly promising and economical technique for predicting the unsteady aerodynamic effects of BVI is the indicial method. The indicial response is defined as the response of the aerodynamic flowfield to a step change in a set of defined boundary conditions (forcing). This can be step change in airfoil angle of attack, a step change in control surface deflection, or an encounter with a sharp-edged gust. With the indicial response, the net response to an arbitrary forcing can be found by Duhamel superposition. If the linearity of the flow over the required range of conditions can be justified on physical grounds, then the advantage of the indicial method is a tre-

Received Feb. 1, 1997; revision received June 12, 1997; accepted for publication June 13, 1997. Copyright © 1997 by the American Institute for Aeronautics and Astronautics, Inc. All rights reserved.

*Associate Professor, Glenn L. Martin Institute of Technology, Department of Aerospace Engineering. Senior Member AIAA.

mendous saving in computational cost over performing many separate flowfield calculations. Furthermore, if the indicial functions can be represented in an appropriate analytic form, then well-established and efficient numerical methods exist for this superposition process.^{12–14} Good reviews of the basic indicial concept are given in Refs. 15 and 16.

For incompressible flow, the indicial lift on a two-dimensional airfoil undergoing a step change in angle of attack has been obtained.¹⁷ A corresponding solution for a stationary sharp-edged gust in incompressible flow has also been obtained.^{18–20} A summary of these results is given in Ref. 21. In helicopter analyses, both the Wagner¹⁷ and Küssner¹⁸ functions are commonly used in conjunction with Duhamel superposition to treat unsteady aerodynamic effects at a blade sectional level. Compressibility effects on these indicial functions are usually included semiempirically.^{22,23}

While the Küssner function provides a basic representation of unsteady aerodynamic effects, at least in incompressible flow, the helicopter BVI problem is more correctly idealized as an airfoil (blade element) encountering a traveling (convecting) vertical gust field. A gust speed ratio can be defined as

$$\lambda = \frac{V}{(V + V_g)} \quad (1)$$

where V is the velocity of the blade element, and V_g is the normal component of the gust (wake) convection velocity relative to the blade element. For a rotor of radius R and translating forward at an advance ratio μ , the local velocity of a blade element situated at a nondimensional distance \bar{r} from the rotational axis is $V = \Omega R(\bar{r} + \mu \sin \psi)$, where ψ is measured from the downstream-pointing blade. The normal assumption made in most rotor aerodynamic analyses is that the tip vortices (and corresponding induced velocity field) are stationary (nonconvecting) with respect to the rotor, so that $\lambda = 1$ everywhere over the rotor disk. However, the self-induced velocities from the trailed vortex wake system result in a continuously changing and nonuniform convection of the induced velocity field with respect to the rotor. This can produce values of λ at the blade element which can be less than or greater than unity. In this case

$$\lambda(\bar{r}, \mu, \psi) = \frac{\bar{r} + \mu \sin \psi}{\bar{r} + \mu(\sin \psi + V_g/\Omega R)} \quad (2)$$

where V_g is equated to the in-plane component of the wake-induced velocity field perpendicular to the blade element, which can be computed using a prescribed or free vortex wake model for a given rotor operating state. Typical results for λ are plotted in Fig. 1 for several radial blade positions on a four-bladed rotor operating at an advance ratio of 0.1. It will be apparent that for these conditions $\lambda \leq 1$ on the advancing

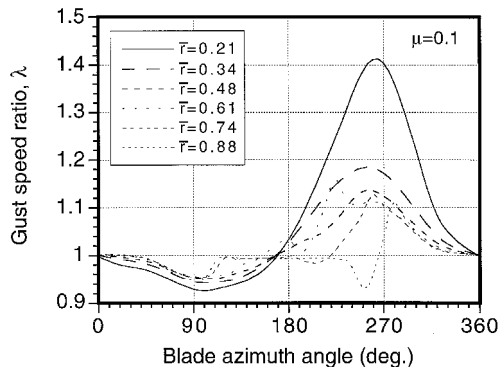


Fig. 1 Typical variation in value of λ for a helicopter blade section at several radial blade stations at an advance ratio of 0.1.

side of the rotor disk and $\lambda \geq 1$ on the retreating side. Note that the deviations from unity (stationary gust field) are largest for the retreating blade ($180 \text{ deg} < \psi < 360 \text{ deg}$) and over the inboard part of the blade.

Numerical results for the lift on a thin two-dimensional airfoil encountering traveling vertical gusts in incompressible flow have been obtained by Miles²⁴ in terms of the parameter λ . Miles²⁴ showed that as the propagation speed of the traveling gust increased from zero to ∞ (λ decreases from 1 to 0), the solution for the lift changes from the Küssner result to the Wagner result, with a variety of intermediate transitional results being obtained. These intermediate results represent the proper indicial functions to use for a general convecting gust analysis, at least if the flow is assumed incompressible. Miles' results²⁴ were later generalized by Drischler and Diederich,²⁵ who obtained continuous semianalytical forms for both the lift and moment gust functions. Both approaches made use of either algebraic or exponential approximations to the Wagner function to facilitate numerical solutions.

Results for traveling gusts for Mach numbers greater than zero are considerably more difficult to obtain, but analytic results for supersonic flows have been obtained by Drischler and Diederich.²⁵ The subsonic case has been examined by Lomax,²⁶ who obtained analytic solutions for the chordwise pressure loading on thin airfoils during the penetration of stationary sharp-edged gusts. Unfortunately, unlike the classical Küssner sharp-edged gust function, there are no equivalent closed-form solutions for the gust available in the subsonic case, and exact analytical expressions for the airfoil pressure distribution can be found only for a limited period of time after the gust entry. The subsonic stationary gust result was also obtained in approximate form as a sum of exponential functions by Heaslet and Spreiter²⁷ using reciprocal relations. Neither author has, however, obtained results for traveling gusts in subsonic flows.

In the present work, an entirely different approach is taken for the calculation of the lift and moment on airfoils encountering traveling gusts. The approach makes use of the reverse flow theorems, which permit the use of known solutions for steady or unsteady airfoil flows and obviate the need to start the problem from first principles. In this paper, solutions for downstream and upstream traveling sharp-edged gusts are obtained, for both incompressible and subsonic compressible flow. The results are also generalized numerically, permitting the airloads for any arbitrary traveling gust field, such as a convecting vortex, to be computed. The overall objective of the work is to provide an improved indicial function representation for use in helicopter rotor aeroacoustic analyses.

Approach

Traveling Sharp-Edged Gust–Boundary Conditions

Consider a two-dimensional airfoil traveling with velocity V and subject to a vertical sharp-edged gust field of magnitude w_0 convecting with velocity $V_g = (\lambda^{-1} - 1)V$. When the gust field is stationary, $\lambda = 1$, and when traveling toward the airfoil at infinite speed, $\lambda = 0$. For the sharp-edged gust, the primary boundary condition is that w is zero on the part of the airfoil that has not reached the gust front. This means that for a downstream traveling gust

$$w = \begin{cases} 0 & \text{if } \zeta > \zeta_0 = V\lambda^{-1}t/c = s/2\lambda \\ w_0 & \text{if } \zeta < \zeta_0 = V\lambda^{-1}t/c = s/2\lambda \end{cases} \quad (3)$$

and for an upstream traveling gust

$$w = \begin{cases} 0 & \text{if } \zeta < \zeta_0 = 1 - V|\lambda|^{-1}t/c = 1 - s/2|\lambda| \\ w_0 & \text{if } \zeta > \zeta_0 = 1 - V|\lambda|^{-1}t/c = 1 - s/2|\lambda| \end{cases} \quad (4)$$

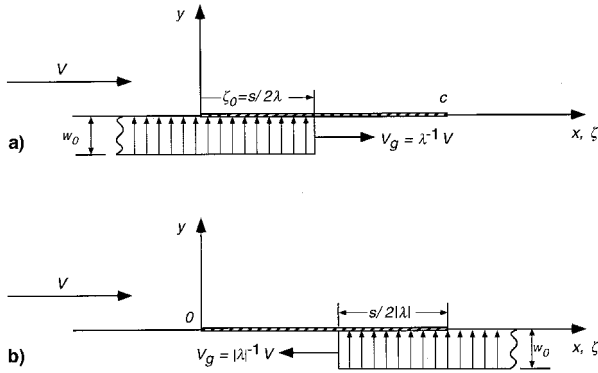


Fig. 2 Sharp-edged gust moving a) downstream relative to airfoil ($\lambda > 0$) and b) upstream relative to airfoil ($\lambda < 0$). Adapted from Miles.²⁴

which is shown in Fig. 2. In either case, it will be seen that the effective angle of attack changes progressively as a function of time as the airfoil penetrates into the gust front. For a stationary gust $\lambda = 1$, and under incompressible flow assumptions, this is equivalent to solving Küssner's problem.^{18,20} For $\lambda = 0$, this is equivalent to Wagner's problem for a sudden change in angle of attack.¹⁷ One objective of the current work is to obtain results for any value of λ , and in a suitable analytic form to permit the calculation of the lift and moment for any arbitrary gust field.

Reverse Flow Theorems

Reciprocal theorems have been applied to many aerodynamic problems (where they are usually called reverse flow theorems).^{27–35} The main utility of the reverse flow theorems is that they build from known solutions for airfoil flows and obviate the need to start each new problem from first principles. They are ideally suited to solving various indicial problems, both analytically and numerically, but surprisingly have not seen widespread use. Nevertheless, they have recently been used by Hariharan and Leishman³⁶ to calculate the indicial responses of airfoils with flaps in subsonic flow. Their utility, however, extends only to the integrated forces and moments on the airfoil, not pressure distributions.

Very general forms of the aerodynamic reverse flow theorems have been established by Heaslet and Spreiter.²⁷ Theorems for the calculation of both the lift and pitching moment are given in Ref. 27 and are applicable to both steady and indicial motion.

Reverse Flow Theorem 1

The lift in steady or indicial motion of one airfoil having arbitrary twist and camber is equal to the integral over the planform of the product of the local angle of attack and the loading per unit angle of attack at the corresponding points on a second flat-plate airfoil of identical planform, but moving in the reverse direction.

The significance of Theorem 1 can be easily illustrated. Consider two airfoils, one moving in a forward direction and the other in a reverse direction. The first airfoil (the unknown problem) has an arbitrary angle of attack distribution $\alpha_1(x_1)$, which could be produced by a gust field or a flap. The second airfoil is a flat plate at constant angle of attack, $\alpha_2 = \text{const}$, which is assumed to have a known aerodynamic loading over the chord. This known loading can be of analytic or numerical form and could be computed by a variety of methods. The boundary conditions are

$$\alpha_1 = \alpha_1(x_1), \quad \alpha_2 = \text{const} \quad (5)$$

The first reverse flow theorem gives the result that

$$\alpha_2 C_{l_1} = \int_1 \alpha_2 \Delta C_{p_1} dx_1 = \int_2 \alpha_1 \Delta C_{p_2} dx_2 \quad (6)$$

In other words, the lift coefficient on the first airfoil can be found from the loading on the second airfoil by integrating the known solution and the local chordwise angle of attack, using

$$C_{l_1} = \int_2 \alpha_1 \left(\frac{\Delta C_{p_2}}{\alpha_2} \right) dx_2 \quad (7)$$

Another set of reverse flow theorems apply for calculating pitching moments. In this case, one has to make use of results for pitch rate motion about some axis.

Reverse Flow Theorem 2

The pitching moment on one airfoil with arbitrary twist and camber is equal to the integral over the planform of the product of the local angle of attack and the loading per unit nondimensional pitch rate at the corresponding points of a second airfoil of the same planform, but comprising a flat plate moving in the reverse direction and pitching about the moment axis of the first airfoil.

In this case, the pitching moment of the first airfoil is given by

$$C_{m_1} = \int_1 \alpha_2 \left(\frac{\Delta C_{p_1}}{q_2} \right) dx_1 = \int_2 \alpha_1 \left(\frac{\Delta C_{p_2}}{q_2} \right) dx_2 \quad (8)$$

The requirement for pitching about the moment axis of the first airfoil introduces some additional complexity to the problem. However, if the known result for the second airfoil is for pitching about its leading edge, then the moment about the leading edge of the first airfoil can be written as

$$C_{m_{le}} = \int_2 \alpha_1 \left(\frac{\Delta C_{p_2}}{q_2} \right) dx_2 - \int_2 \alpha_1 \left(\frac{\Delta C_{p_2}}{\alpha_2} \right) dx_2 \quad (9)$$

which makes use of the chordwise loading solutions for both angle of attack and pitch rate. The moment about the 1/4 chord or any other axis can then be obtained by a simple transformation. Therefore, the reverse flow theorems allow the steady or unsteady lift and moment for any set of boundary conditions to be simply obtained from the steady or unsteady results on a flat-plate airfoil.

Results and Discussion

Traveling Sharp-Edged Gusts-Incompressible Flow

The reverse flow theorems will now be applied to solve the traveling sharp-edge gust problem in an incompressible flow. For $M = 0$, the chordwise pressure loading for an indicial change in angle of attack is given by¹⁵

$$\frac{\Delta C_p(\zeta, t)}{\alpha} = \frac{4}{V} \delta(t) \sqrt{(1-\zeta)\zeta} + 4\phi_w(s) \sqrt{\frac{1-\zeta}{\zeta}} \quad (10)$$

The corresponding result for an indicial change in pitch rate about the leading edge is given by¹⁵

$$\begin{aligned} \frac{\Delta C_p(\zeta, t)}{q} = & \frac{\delta(t)}{V} (1 + 2\zeta) \sqrt{(1-\zeta)\zeta} \\ & + (3\phi_w(s) - 1) \sqrt{\frac{1-\zeta}{\zeta}} + 4\sqrt{(1-\zeta)\zeta} \end{aligned} \quad (11)$$

Note that the first term in each of the two preceding equations is the noncirculatory or apparent mass loading, which for the incompressible case is in the form of a Dirac delta function.

By using the reverse flow theorems, the time-varying (indicial) lift on the airfoil for a traveling sharp-edged gust can be obtained by integration of the known flat-plate indicial pressure loading over the appropriate part of the airfoil affected by the gust front, but when moving in the reverse direction. For the downstream traveling gust, this is equivalent to integrating the known flat-plate loading from the trailing edge to the leading edge of the gust front at ζ_0 (Fig. 2). For the upstream traveling gust, the known loading must be integrated from the leading edge of the airfoil up to ζ_0 . It will be immediately apparent that different results, both quasisteady and indicial, will be produced for downstream vs upstream moving gusts.

For incompressible flows, the noncirculatory part of the unsteady lift can be written in terms of the instantaneous upwash over the airfoil. For a traveling sharp-edged gust, results can be obtained analytically by the integration of the first term of Eq. (10) with the boundary conditions given in Eqs. (3) and (4). For a downstream traveling gust, the noncirculatory lift can be shown to be

$$\frac{C_n^{nc}(t)}{(w_0/V)} = \frac{\partial}{\partial t} \left(\frac{\sin 2\theta_0}{2} - \theta_0 + \pi \right) / 2 \quad (12)$$

where $\theta_0 = \cos^{-1}(1 - 2\zeta_0)$, so that $\theta_0 = 0$ at the time when the gust front is at the airfoil leading edge and $\theta_0 = \pi$ at the trailing edge. For the upstream traveling sharp-edged gust, the corresponding result for the noncirculatory lift is

$$\frac{C_n^{nc}(t)}{(w_0/V)} = \frac{\partial}{\partial t} \left(\theta_0 - \frac{\sin 2\theta_0}{2} \right) / 2 \quad (13)$$

Eqs. (12) and (13) can be evaluated numerically at discrete values of time as the gust front proceeds over the airfoil, the time derivatives being evaluated by means of finite differences.

Unlike the apparent mass terms, the circulatory parts of the unsteady lift depend on the prior time history of the gust field, and so the lift must be obtained by Duhamel superposition. For a downstream traveling gust, the quasisteady part of the circulatory lift can be obtained analytically by integration of the second term in Eq. (10) with the appropriate boundary conditions. For the downstream traveling sharp-edged gust, it can be shown that the quasisteady circulatory lift is

$$\frac{C_l^{qs}}{(w_0/V)} = 2(\pi - \theta_0 - \sin \theta_0) \quad (14)$$

or in terms of equivalent angle of attack

$$\frac{C_l^{qs}}{(w_0/V)} = 2\pi\alpha^{qs} = 2\pi \left(1 - \frac{\theta_0}{\pi} - \frac{\sin \theta_0}{\pi} \right) \quad (15)$$

For the upstream traveling sharp-edged gust, the equivalent quasisteady angle of attack is

$$\alpha^{qs} = \left(\frac{\theta_0}{\pi} + \frac{\sin \theta_0}{\pi} \right) \left(\frac{w_0}{V} \right) \quad (16)$$

The net unsteady circulatory lift must now be determined by linear superposition, that is, using Duhamel superposition with the instantaneous or quasisteady equivalent angle of attack and the Wagner function. Duhamel's superposition integral can be written analytically as

$$C_l^c(s) = 2\pi \left[\alpha^{qs}(0+) \phi_w(s) + \int_{0+}^s \frac{\partial \alpha^{qs}}{\partial t} \phi_w(s - \sigma) d\sigma \right] \quad (17)$$

and this can be solved numerically with a suitable algebraic or exponential form for ϕ_w . For example, if Jones' exponential approximation³⁴ for the Wagner function is assumed, i.e.,

$$\phi_w(s) = 1 - \sum_{i=1}^N A_i \exp(-b_i s) \quad s > 0^+ \quad (18)$$

with $N = 2$ and $A_1 = 0.33$, $A_2 = 0.67$, $b_1 = 0.0455$, and $b_2 = 0.3$, e.g., Ref. 21, then a finite difference approximation to the Duhamel integral leads to a one-step recursive formulation. Denoting the current time step by t , the net lift coefficient C_l can be found using

$$C_l^c = 2\pi \left(\alpha^{qs} - \sum_{i=1}^N Z_i \right) = 2\pi \alpha_{e_i} \quad (19)$$

where the Z_i or deficiency terms are given by the one-step recursive formulas

$$Z_i = Z_{i-1} E_i + A_i (\alpha_t^{qs} - \alpha_{t-1}^{qs}) \quad (20)$$

with $E_i = \exp(-b_i \Delta s)$. The subscripts t and $t-1$ are the current and previous time steps, respectively. The deficiency functions Z_i contain all of the time-history information and are simply updated once at each time step as the airfoil penetrates into the gust front.

The calculation of the corresponding unsteady pitching moments proceeds by a similar process. This case is somewhat more difficult because the chordwise loading as a result of pitch rate must be used in addition to the angle of attack result, see reverse flow Theorem 2. However, a simplifying result is noted in this case if one recognizes that if the moment axis is taken about the quarter-chord, then all terms involving the Wagner function disappear. This eliminates the need to perform any further Duhamel superposition, leaving only integrals involving quasisteady and apparent mass terms. In the case of a downstream traveling gust, the unsteady pitching moment about the quarter-chord is

$$\frac{C_m^{nc}(t)}{(w_0/V)} = \frac{\partial}{\partial t} \left[\frac{3}{8} \left(\theta_0 - \frac{\sin 2\theta_0}{2} - \pi \right) + \frac{\sin^3 \theta_0}{12} \right] \quad (21)$$

and for an upstream traveling gust

$$\frac{C_m^{nc}(t)}{(w_0/V)} = \frac{\partial}{\partial t} \left[\frac{3}{8} (\sin 2\theta_0 - \theta_0) - \frac{\sin^3 \theta_0}{12} \right] \quad (22)$$

Results for the unsteady lift and pitching moment for downstream traveling sharp-edged gusts are shown in Fig. 3. For $\lambda = 0$ ($V_g = \pm\infty$), the results are shown to lead to the Wagner function, with the formation of the singular part [a Dirac delta function of magnitude $\delta(t)/2$ at $s = 0$], and, thereafter, a growth in lift from half its final value at $s = 0^+$. Perhaps more significantly, note that for $\lambda = 1$ ($V_g = 0$), the present results reduce to the Küssner function, which grows from zero lift at $s = 0$. These two results are shown in Fig. 4 and have been compared with the tabulations of these functions given by Sears²⁰ or Lomax,¹⁵ for which the agreement is essentially exact.

For intermediate values of λ , an interesting series of results are obtained as the gust propagation speed increases from zero ($\lambda = 1$). As shown in Fig. 5, which presents a breakdown of the constituent parts of the lift, the noncirculatory term is responsible for the very large peaks in the lift produced as λ decreases. The lift reaches a maximum at the point when the airfoil is about halfway into the gust. It can be seen that the magnitude of these peaks is often larger than the steady-state lift coefficient of 2π per radian. For gusts that move with the wing at velocities less than 0 ($\lambda > 1$), the noncirculatory part

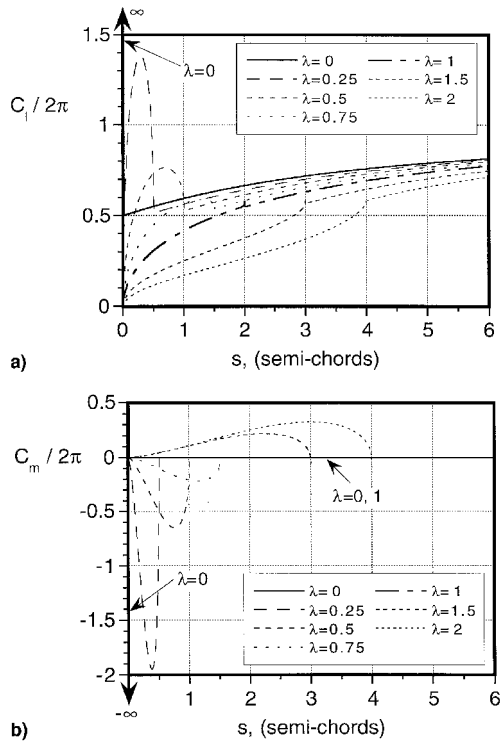


Fig. 3 a) Lift and b) moment for downstream-moving sharp-edged gusts in incompressible flow.

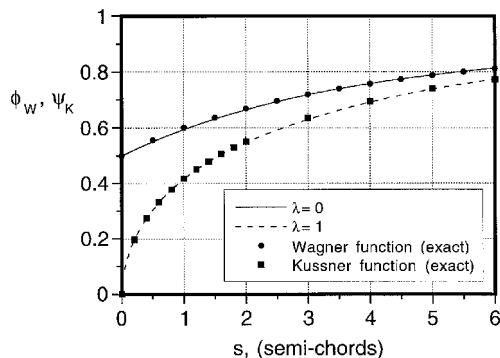


Fig. 4 Numerical calculation of Küssner's function using reverse flow theorems compared to exact solution.

of the lift is small and the circulatory lift grows only very slowly with time.

The corresponding pitching moment for downstream traveling gusts also shows an interesting and significant behavior (Fig. 3), with a change in the sign of the c.p. for λ greater or less than 1. For the stationary gust ($\lambda = 1$), the c.p. remains at the quarter-chord throughout the motion, a result previously proved analytically by Sears.²⁰ As the gust speed approaches infinity, the peak in the moment approaches $-\pi\delta(t)$ with the c.p. moving to midchord. For receding gusts, the c.p. moves in front of the quarter-chord.

Results for upstream traveling gusts are shown in Fig. 6. Again, for large gust velocities the results approach the Wagner function. For progressively slower gusts, large peaks in the lift and moment appear as a result of the noncirculatory contributions to the airfoil loading. Note that the noncirculatory terms are the same for any value of $|\lambda|$, but that the total transient value of the lift is higher than for a downstream traveling gust. The reasons for this will be apparent from a comparison of Eqs. (15) and (16), which simply prove that a gust affecting the trailing edge of the airfoil will have a larger effect on the circulatory lift than a gust affecting the same percentage of the leading edge. For the same reason, a trailing-edge flap

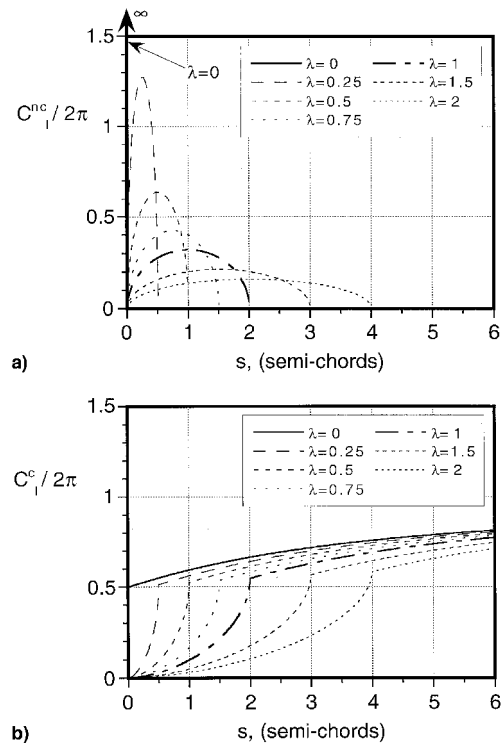


Fig. 5 Apparent a) mass and b) circulatory contributions to the unsteady lift for downstream-moving sharp-edged gusts in incompressible flow.

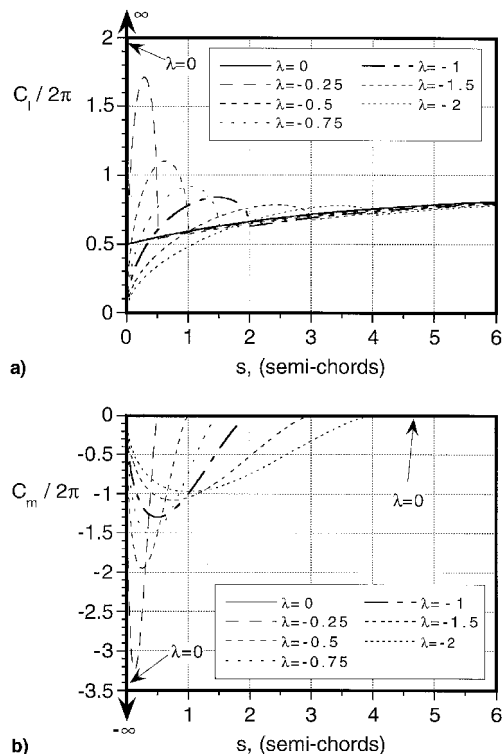


Fig. 6 a) Lift and b) moment for upstream-moving sharp-edged gusts in incompressible flow.

deflection is more effective in producing a change in lift than a leading-edge flap.

BVI Predictions-Incompressible Flow

The foregoing results have illustrated the significant effects of the gust speed ratio on the unsteady lift and moment for a sharp-edged gust. In the sharp-edged gust case, semiexact re-

sults have been obtained because certain integrals can be evaluated analytically. For the general case, the distribution of w will be nonuniform over the airfoil chord, and although the reverse flow theorems can still be employed, the chordwise integrals cannot be found analytically.

One such case with a general downwash distribution across the chord involves the interaction of a vortex with an airfoil. This is a classical and very practical problem in unsteady aerodynamics but apparently has not been solved for nonstationary or convecting vortices in incompressible flow, that is, for $\lambda \neq 1$. For the stationary vortex, the time-varying lift can be obtained by Duhamel superposition with the Küssner function, and the moment about the quarter-chord remains zero throughout.²⁰ This result follows from the present work as a special case.

To solve for the lift and moment for this general downwash problem, a series of control points were distributed across the airfoil chord. While the evaluation of the downwash at many points over the chord is not desirable for a rotor analysis, the incompressible theory furnishes a means of obtaining results free from any approximations other than to the Wagner function. The induced angle from a desingularized vortex of unit strength ($\Gamma/V_\infty c = 1$), convecting one chord ($h = c$) below the airfoil, was computed for a series of gust speed ratios. The normal component of velocity induced on the airfoil by the vortex is

$$w(x, t) = \frac{\Gamma(x - x_v)}{2\pi(r_c^2 + r^2)} \quad (23)$$

where r is the distance along a radial from the vortex center such that $r^2 = (x - x_v)^2 + (y - h)^2$. The core radius r_c was assumed to be $0.05c$. At each time step, the downwash over the airfoil was computed and all of the integrals necessary to compute the apparent mass and circulatory terms were evaluated numerically.

Results for the lift and moment are shown in Fig. 7 as a function of time in semichords of airfoil travel. The results are referenced such that $s = 0$ when the stationary vortex is at the airfoil leading edge. Note the familiar lift response for a BVI

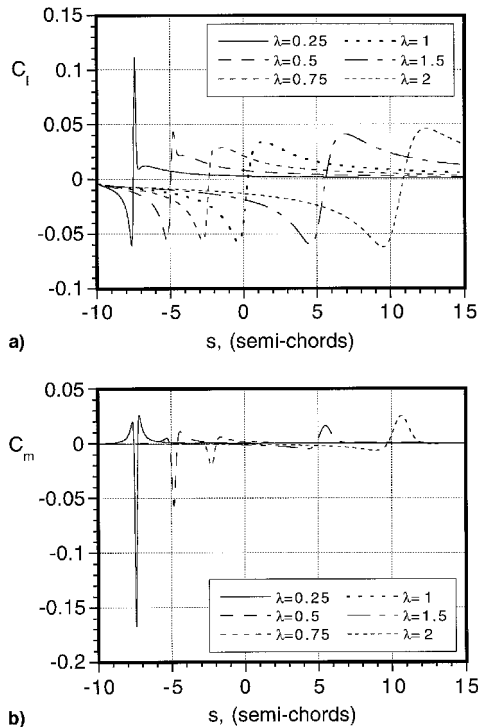


Fig. 7 Predictions of a) lift and b) moment for downstream-conducting vortices in incompressible flow.

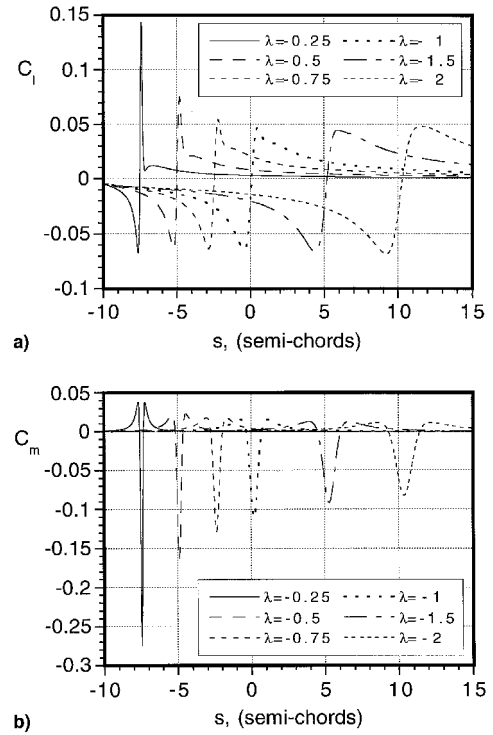


Fig. 8 Predictions of a) lift and b) moment for upstream-conducting vortices in incompressible flow.

event, with a reduction in lift as the vortex approaches the airfoil, a rapid change and growth in lift as the vortex core crosses below the chord, followed by a slow reduction in lift as the vortex convects downstream. The effects of gust speed ratio on the induced airloads were found to be significant, with the time-rate-of-change of lift on the airfoil increasing as V_g increased. At the same time, the interaction occurs earlier or later in time relative to the baseline (stationary) vortex.

Of particular note in Fig. 7 is the effect of gust speed ratio on the pitching moment. For $\lambda < 1$ ($V_g > 0$), the c.p. is aft of the quarter-chord and a negative going moment pulse is obtained. This is a result of the noncirculatory terms beginning to dominate the solution, which have centroids other than the quarter-chord. For $\lambda > 1$ ($V_g < 0$), the noncirculatory terms are small and the c.p. moves forward of the quarter-chord, thereby giving a positive pitching moment in the initial stages.

Equivalent results for upstream traveling vortices are shown in Fig. 8. The lift and moment are again noted to be more sensitive to upstream traveling gust fields. Because of the sensitive effects of λ on the BVI airloads, it is instructive to examine the effects on the acoustics. The Ffowcs-Williams-Hawkins equation shows that in the far-field compact source limit, the acoustic pressure resulting from the airfoil loading is proportional to the time-rate-of-change of lift.^{3,4,37} Acoustic pressure results for the downstream traveling vortices are shown in Fig. 9, the results being unscaled because no directional path to an observer has been specified. While the overall shape of the acoustic pressure pulse is the same, the sensitivity of its magnitude to the gust speed ratio is clearly very significant.

Traveling Sharp-Edged Gusts-Subsonic Flow

The stationary sharp-edged gust problem in subsonic flow has been tackled by Lomax²⁶ and is also summarized in Ref. 21. For the early period $0 \leq s \leq 2M/(1 + M)$, the lift and moment vary as simple polynomials. For the lift, Lomax²⁶ gives

$$C_l(s) = \frac{2s}{\sqrt{M}} \left(\frac{w_0}{V} \right) \quad (24)$$

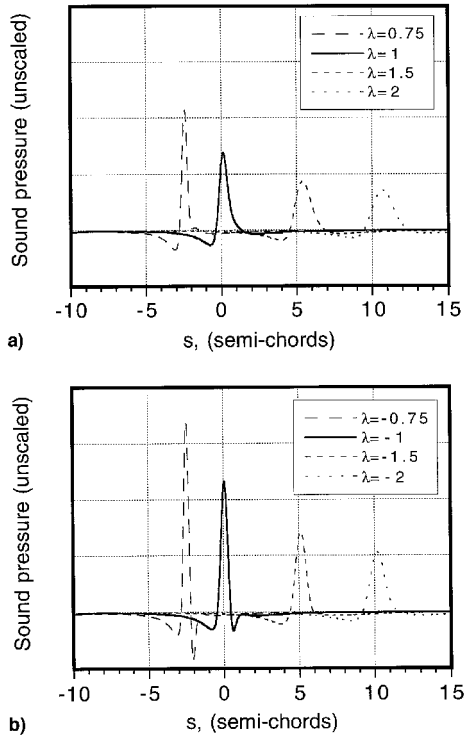


Fig. 9 Predictions of acoustic pressure for nonstationary vortices in incompressible flow: a) downstream and b) upstream traveling vortices.

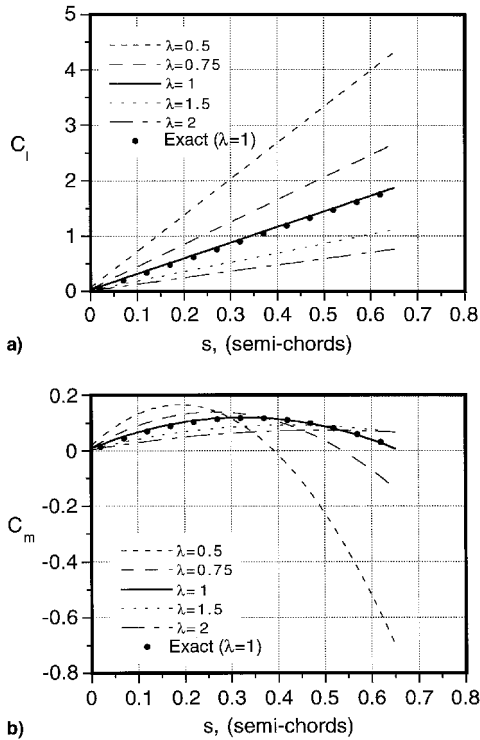


Fig. 10 a) Lift and b) moment for downstream-moving sharp-edged gusts in subsonic flow at $M = 0.5$, as given by exact linear theory.

The pitching moment can be deduced from Ref. 21 and is

$$C_m(s) = \frac{1}{2\sqrt{M}} \left[s - \left(\frac{M+1}{2M} \right) s^2 \right] \left(\frac{w_0}{V} \right) \quad (25)$$

For later values of time, the results are too complicated to be

found analytically, although some numerical results are still possible.²⁶

Lomax's results²⁶ for the gust case can also be obtained and verified by use of the reverse flow theorems and further extended to traveling gusts by analogy with the incompressible results given previously. In the subsonic case, the exact solution for the chordwise pressure loading on an airfoil undergoing a unit step change in angle of attack is³⁸

$$\begin{aligned} \frac{\Delta C_p^\alpha(x, \hat{t})}{\alpha} = \Re \left(\frac{8}{\pi(1+M)} \sqrt{\frac{\hat{t}-x'}{\hat{t}+x'}} \right. \\ \left. + \frac{4}{\pi M} \left\{ \cos^{-1} \left[\frac{\hat{t}(1+M) - 2(c-x')}{\hat{t}(1-M)} \right] \right. \right. \\ \left. \left. - \cos^{-1} \left[\frac{2x' - \hat{t}(1-M)}{\hat{t}(1+M)} \right] \right\} \right) \quad (26) \end{aligned}$$

where the domain is $x' = x - M\hat{t}$. Also, the exact solution for the chordwise pressure on an airfoil undergoing a unit step change in pitch rate about the leading edge is

$$\begin{aligned} \frac{\Delta C_p^\alpha(x, \hat{t})}{q} = \Re \left[\frac{8}{\pi M c} \left(\sqrt{(\hat{t}-x')(M\hat{t}+x')} \right. \right. \\ \left. \left. + \frac{M(1-M)}{3(1+M)^2} \sqrt{\frac{(\hat{t}-x')^3}{(M\hat{t}+x')}} \right. \right. \\ \left. \left. - \sqrt{(c-M\hat{t}-x')(\hat{t}+x'-c)} \right. \right. \\ \left. \left. + \frac{1}{2} (M\hat{t}+x') \left\{ \cos^{-1} \left[\frac{\hat{t}(1+M) - 2(c-x')}{\hat{t}(1-M)} \right] \right. \right. \right. \\ \left. \left. \left. - \cos^{-1} \left(\frac{2x' - \hat{t}(1-M)}{\hat{t}(1+M)} \right) \right\} \right) \right] \quad (27) \end{aligned}$$

where both equations are valid for the early period $0 \leq \hat{t} \leq c/(1+M)$. Note that \Re refers to the real part, where the real parts of the arc cosine of numbers greater than 1 and less than -1 are 0 and π , respectively.²⁶ Also, in contrast to the incompressible case, at time zero the initial loading for each mode of forcing is finite as given by piston theory.²¹

The subsonic values of lift and moment for the penetration of a traveling sharp-edged gust can only be found by numerical means. In this case, however, in addition to chordwise integration of the loading over the appropriate part of the chord by means of the reverse flow theorems, the time-history of the loading must be accounted for by Duhamel superposition. For example, the lift can be written as

$$c_l(s) = \int_0^s \int_0^{\hat{t}_0} \Delta C_p(\zeta = s/2|\lambda| - \sigma, s - \sigma) d\zeta d\sigma \quad (28)$$

which is solved numerically, and where the chordwise integration of the flat-plate loading is performed for downstream or upstream traveling gusts over the appropriate part of the chord in accordance with the reverse flow theorems.

Results for the lift and quarter-chord moment on the airfoil penetrating sharp-edged gusts at a Mach number of 0.5 are shown in Fig. 10 for various gust speed ratios. Results at other Mach numbers are qualitatively similar and are not shown here for brevity. The exact solutions for $\lambda = 1$, as given by Eqs. (24) and (25), are found to agree precisely with the numerical results. The effect of increasing gust velocity is to increase the rate of buildup of lift, analogous to the incompressible case. Unfortunately, results can only be computed for up to $s = 2M/(1+M)$ but vividly illustrate the sensitivity of

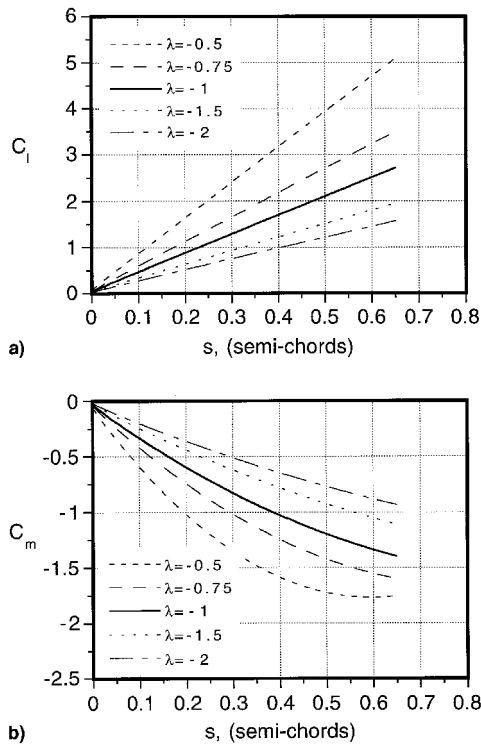


Fig. 11 a) Lift and b) moment for upstream-moving sharp-edged gusts in subsonic flow at $M = 0.5$, as given by exact linear theory.

the gust speed ratio on the aerodynamic response. For the subsonic case, the c.p. is always initially forward of the quarter-chord as the airfoil penetrates into the gust front but moves back quickly again after the airfoil becomes fully immersed in the gust. For large values of time, the aerodynamic center ultimately moves to the quarter-chord.

Computed results for upstream traveling gusts at a Mach number of 0.5 are shown in Fig. 11. Analogous to the incompressible case, the upstream traveling gust produces a more rapid growth in lift. Also, in this case the initial moment is significantly nose down, again analogous to the incompressible case. However, compared to the incompressible case, in the subsonic case both the magnitude and time-history of the moments are quite different.

Direct Simulation by Euler Method

Modern finite difference-based solutions can help establish results for many practical problems that would otherwise remain intractable by analytic means. However, these solutions are only available at significant computational cost and even then are subject to certain approximations and limitations. Indicial-type calculations are extremely useful, but it is difficult to obtain reliable results because of the need to use fine grids and small time steps.³⁹ Recent works by Parameswaran⁴⁰ and Singh and Baeder⁴¹ have shown the ability to compute accurately indicial solutions using an Euler method with a grid-velocity approach for representing the transient changes in the boundary conditions. The pressure distributions and integrated airloads have been compared in Ref. 41 with exact solutions given by linear theory for indicial changes in angle of attack and pitch rate, with excellent correlation. The exact results from linear theory help provide validation for the Euler method and also good check cases for the indicial method over a range of conditions where analytical solutions may be unavailable.

Lift and pitching moment results for traveling sharp-edged gusts have also been computed using the Euler method. The airfoil used was a NACA 0006 and a vertical gust velocity

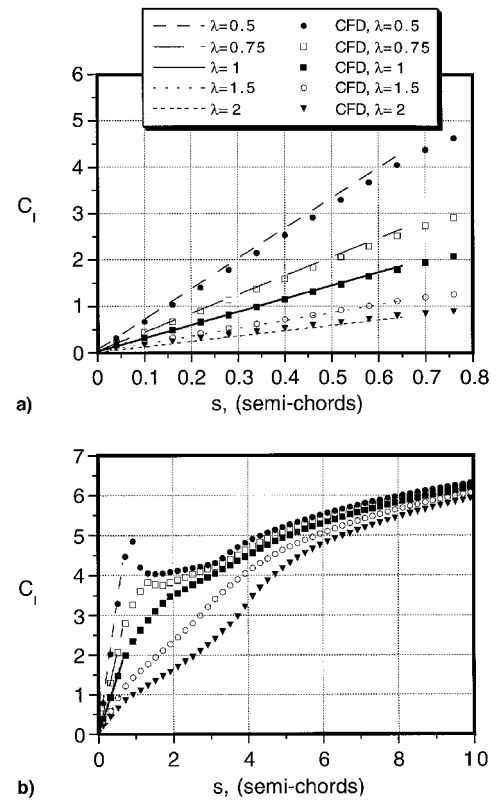


Fig. 12 Euler calculations of unsteady lift for downstream-moving nonstationary sharp-edged gusts at $M = 0.5$ and comparisons to exact linear theory: a) early and b) later values of time.

equivalent to a net 2-deg change in angle of attack was assumed. Euler results for convecting sharp-edged gusts are shown in Fig. 12 for a Mach number of 0.5 and for several gust speed ratios. Note that in the early period, where $s < 2M/(1+M)$, or 0.67 semichords at this Mach number, the lift varies linearly with time as predicted by the exact linear theory, the rate of growth increasing with increasing gust convection velocity. The comparisons are excellent and lend significant credibility to the Euler results, which can provide solutions for later values of time where exact solutions are not possible. Like the incompressible results, the Euler results predict an initial lift overshoot for $s > 2M/(1+M)$ that reaches a peak when the airfoil is about halfway into the gust.

Corresponding results for the pitching moment are shown in Fig. 13. Again, the results computed using the Euler method are in excellent agreement with the linear theory at small values of time. As $\lambda \rightarrow 0$, the initial value of the pitching moment approaches a pulse of magnitude $-1/M$, as given by the piston theory.²¹ Of particular interest here is the behavior of the pitching moment at later values of time, a result that cannot be established from the linear theory. It is apparent from the Euler results that the c.p. again moves forward of quarter-chord after the airfoil fully penetrates the gust front and ultimately asymptotes to near quarter-chord only at relatively large values of time ($s > 6$).

Approximations to Gust Function

In any practical application of indicial theory, the gust functions must be represented in a convenient analytic form for all values of s to permit Duhamel superposition. As shown previously, while the incompressible case can be dealt with in a semiexact form (except for the approximation to the Wagner function), the subsonic case is not known analytically for $s > 2M/(1+M)$. Therefore, the problem must be handled by a direct curve fit to the lift time-history for the traveling sharp-edged gust as computed using the Euler method.

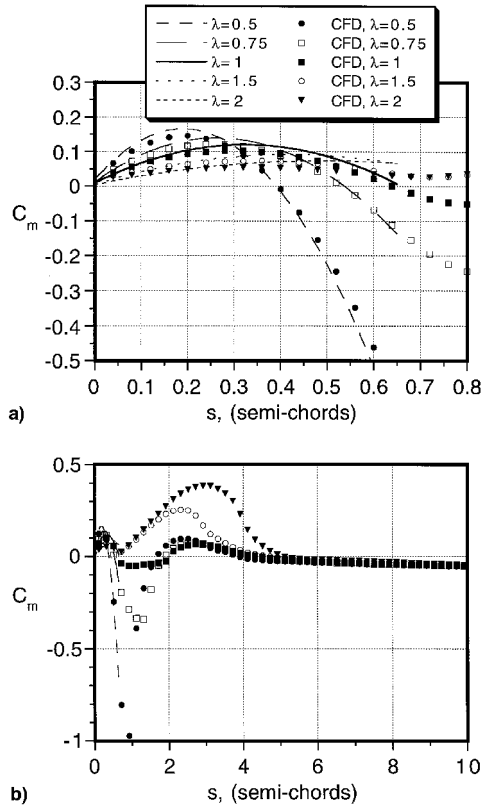


Fig. 13 Euler calculations of unsteady moment about quarter-chord for downstream-moving nonstationary sharp-edged gusts at $M = 0.5$ and comparisons to exact linear theory: a) early and b) later values of time.

An exponential fit to the indicial function will be used because it lends itself easily to numerical superposition by Duhamel's principle in the form of the one-step recursive solution given previously by Eq. (19). Mazelsky,⁴² and Mazelsky and Drischler⁴³ obtained exponential approximations to the stationary sharp-edged gust function, but not for traveling gusts. While the exponential behavior of the indicial function is not an exact representation of the physical behavior, it is usually sufficiently close for practical calculations. However, for some applications, the exponential approximation to the indicial response may not be adequate, and caution should always be used.

An exponential approximation to the lift produced on an airfoil encountering a traveling sharp-edged gust is assumed to be of the form

$$\frac{C_l(s)}{w_0/V} = C_{l_a}(M) \left(1 - \sum_{i=1}^N G_i \exp(-g_i s) \right) + G_{N+1} \exp(-g_{N+1} s) - G_{N+1} \exp(-g_{N+2} s) \quad s \geq 0 \quad (29)$$

where all of the coefficients will, in general, be Mach number-dependent. To satisfy the initial conditions at $s = 0$, then $\sum_{i=1}^N G_i = 1$. Also, $g_i > 0$ for $i = 1 \dots N + 2$. The transient shown in the lift response at small values of time for fast traveling gusts is represented by the last two terms in Eq. (29), where the coefficient G_{N+1} and the differences in the values of the time constants g_{N+1} and g_{N+2} will affect the size and width of this transient. Physically, this transient is a result of the accumulation of pressure waves. In the limit when $\lambda \rightarrow 0$, the magnitude of the transient approaches the piston theory value of $4/M$.

The functional form of Eq. (29) was fitted in a least-squares sense to the Euler results. This was done by setting up the solution as an optimization problem with equality constraints

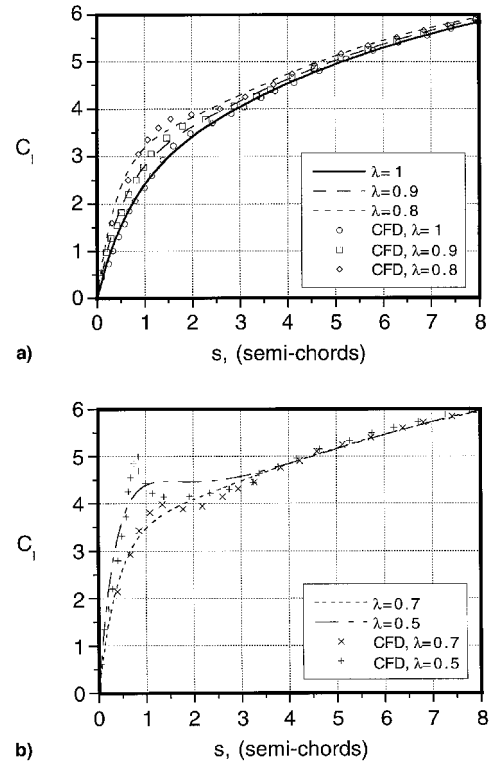


Fig. 14 Exponential curve fits to Euler results for traveling sharp-edged gusts, $M = 0.5$.

and minimizing the cost function. Typically, four exponential terms ($N = 4$ or 7 coefficients) were found necessary to represent the traveling gust functions to an acceptable degree of accuracy. Results of this curve-fitting process are shown in Fig. 14 for several gust speed ratios at a Mach number of 0.5. It is seen that while an exact fit to the initial transient at smaller values of λ cannot be obtained, an acceptable level of accuracy is possible for acoustically significant values of λ , that is, $\lambda < 1$ (corresponding to the advancing blade). The generalization of these gust functions in terms of λ is, however, left as a future task.

Subsonic BVI Problem

The final results presented in this article are for the airloads and noise generated by an airfoil encountering a convecting vortex in subsonic flow. Again, the compact source assumption is used so that the noise results are valid only for the far field. Most of the BVI noise generated by helicopter rotors occurs on the advancing side of the disk, and so attention is again placed on downstream traveling gusts so that $\lambda < 1$ ($V_g > 0$). A vortex of strength $\Gamma/V_\infty c = 0.2$ was assumed to convect at a distance of a quarter-chord below the blade. This is a standard test case that has received considerable attention in the literature.^{9,44} The present results were computed by Duhamel superposition using the exponential approximation to the traveling sharp-edge gust function. In this case, Eq. (19) can be modified to read

$$C_{l_t} = C_{l_a}(M) \left(\frac{w_{le}}{V} - Z_{1_t} - Z_{2_t} \right) + \left(\frac{w_{le}}{V} \right) (Z_{3_t} - Z_{4_t}) \quad (30)$$

where w_{le} is the vortex-induced velocity at the airfoil leading edge at t .

Results for the unsteady lift and acoustics are shown in Fig. 15 for several gust speed ratios. Again, the results are all referenced to the $\lambda = 1$ case, so that for downstream traveling vortices the BVI encounter occurs progressively earlier. It will be seen that the effect in increasing vortex convection speed

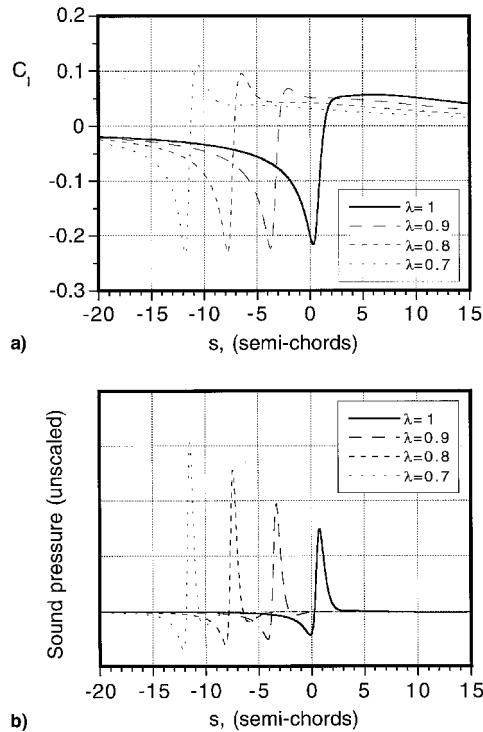


Fig. 15 a) Unsteady lift and b) acoustic pressure for downstream-convecting vortices. $\Gamma/V_\infty c = 0.2$, $h = -0.25c$, and $M = 0.5$.

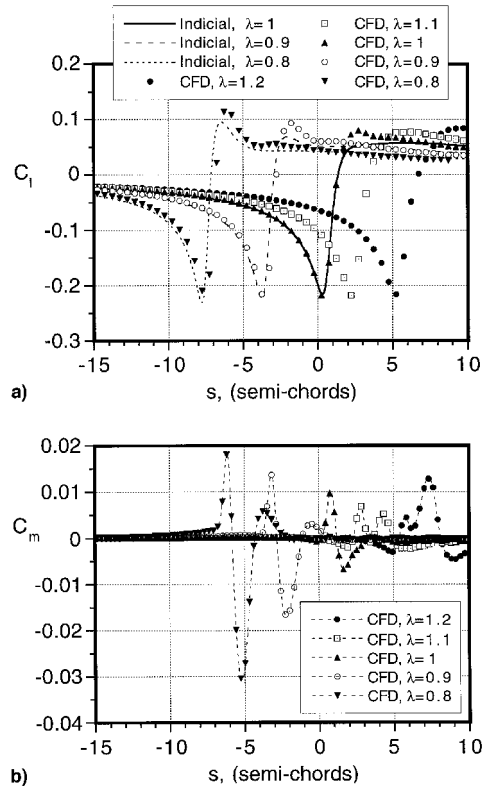


Fig. 16 Indicial and Euler predictions of a) unsteady lift and b) pitching moment for convecting vortices. $\Gamma/V_\infty c = 0.2$, $h = -0.25c$, and $M = 0.5$.

(decreasing λ) is to progressively increase the peak-to-peak value of the unsteady lift but, more importantly, to increase the time-rate-of-change of lift. This latter fact is vividly reflected in the acoustics, where the BVI sound pulse increases significantly in magnitude, even for values of λ not much lower than unity.

Figure 16 shows results for the same BVI problem as computed directly using the Euler method. Results for both $\lambda < 1$ and $\lambda > 1$ are shown. Predictions of the unsteady lift using the indicial method are shown for $\lambda = 0.8, 0.9$, and 1.0 , based on the exponential fits to the sharp-edged gust results given previously in Fig. 14. It can be seen that the correlation of the indicial results with the direct Euler solution is excellent. It is important to note that the computational cost of the indicial method is approximately five orders of magnitude less than the Euler solution. Corresponding results for the pitching moment are also shown in Fig. 16 using the Euler method, although in this case, indicial results have not yet been obtained. For $\lambda = 1$, the moment is small, as might be expected on the basis of the results shown in Fig. 13 and the results for the incompressible BVI problem shown in Fig. 7. It is significant to note that for $\lambda < 1$, a negative-going primary moment peak is obtained, but for $\lambda > 1$, the sign of the primary moment changes, which is consistent with the incompressible results shown in Fig. 7. However, for the subsonic case, the quantitative results are obviously rather different from those of the incompressible case. Overall, these results indicate that the gust speed ratio will be a necessary parameter to account for in helicopter airloads and acoustics analyses.

Concluding Remarks

The lift and moment responses on two-dimensional airfoils encountering traveling sharp-edged gusts have been calculated. The approach has made use of the reverse flow theorems, which have allowed results to be computed requiring only the known loading on flat-plate airfoils undergoing indicial motion. Results for downstream and upstream moving gusts have been computed, both for incompressible as well as linearized subsonic flow.

Overall, the results have shown that the gust speed has a large effect on the lift and moment. For the incompressible flow case, exact results have been computed for all values of time. Large peaks in the airloads exist at small values of time just after the airfoil penetrates the gust front. These peaks can be in excess of the final value of the airloads. In the subsonic case, exact results can be computed only for limited values of time after entering the gust, but the growth in lift has been shown to be much more rapid with increasing gust convection speed. Results for later values of time have been computed using an Euler finite difference method, which have shown qualitatively the same trends as for the incompressible case.

The results have been generalized numerically by means of Duhamel superposition to deal with gusts of arbitrary form. A model problem of a two-dimensional vortex interacting with an airfoil has been examined. The lift and moment for the incompressible case have been solved directly, whereas for the subsonic case exponential fits to the traveling gust functions have been assumed. For this model BVI problem, good agreement has been obtained between the indicial method and results obtained from an Euler method. Furthermore, a cost saving of over five orders of magnitude makes the indicial method computationally very attractive. Overall, the results have indicated that the lift, moment, and acoustic signature are sensitive to the vortex (gust) speed ratio, particularly in the subsonic case.

Acknowledgments

The author would like to thank Rajneesh Singh and James Baeder for providing the sharp-edged gust results using the Euler method. This work was supported by the U.S. Army Research Office under the 1996 MURI on Advanced Active Control of Rotorcraft Vibration and Acoustics. Gary Anderson and Tom Doligalski were the Technical Monitors. The author would like to acknowledge the reviewers of this paper for their useful suggestions.

References

- ¹Johnson, W., "Calculation of Blade-Vortex Interaction Airloads on Helicopter Rotors," *Journal of Aircraft*, Vol. 26, No. 5, 1989, pp. 470–475.
- ²Lorber, P. F., "Blade-Vortex Interaction Data Obtained from a Pressure Instrumented Model Rotor," *Proceedings of the AHS/RAES Technical Specialists Meeting of Rotorcraft Acoustics and Fluid Dynamics* (Philadelphia, PA), American Helicopter Society, Alexandria, VA, 1991.
- ³Schmitz, F. H., and Yu, Y. H., "Helicopter Impulsive Noise: Theoretical and Computational Status," *Journal of Sound and Vibration*, Vol. 109, No. 3, 1986, pp. 361–422.
- ⁴Schmitz, F. H., "Rotor Noise," *Aeroacoustics of Flight Vehicles: Theory and Practice*, Vol. 1, NASA RP 1258, Aug. 1991, Chap. 2.
- ⁵Widnall, S., "Helicopter Noise due to Blade-Vortex Interaction," *Journal for the Acoustical Society of America*, Vol. 50, No. 1 (Pt. 2), 1971, pp. 354–365.
- ⁶Nakamura, Y., "Prediction of Blade-Vortex Interaction Noise from Measured Blade Pressure Distributions," Paper 32, *Proceedings of the 7th European Rotorcraft Forum*, Garmish-Partenkirchen, FRG, 1981.
- ⁷Brentner, K. S., "Prediction of Helicopter Rotor Discrete Frequency Noise," NASA TM 87721, Oct. 1986.
- ⁸Srinivasan, G. R., and McCroskey, W. J., "Numerical Simulations of Unsteady Airfoil Interactions," *Vertica*, Vol. 11, No. 1/2, 1987, pp. 3–28.
- ⁹Baeder, J. D., "Computation of Non-Linear Acoustics in Two-Dimensional Blade-Vortex Interactions," Paper 16, *Proceedings of the 13th European Rotorcraft Forum* (Arles, France), 1987.
- ¹⁰Johnson, W., "A Comprehensive Analytical Model of Rotorcraft Aerodynamics and Dynamics," NASA TM-81182, June 1980.
- ¹¹Yu, Y. H., Gmelin, B., Heller, H., Philippe, J. J., Mercker, E., and Preisser, J. S., "Higher Harmonic Control Aeroacoustics Test—The Joint German/French/US HART Project," 20th European Rotorcraft Forum, Amsterdam, The Netherlands, Oct. 1994 (Paper 115).
- ¹²Edwards, J. W., Ashley, H., and Breakwell, J. V., "Unsteady Aerodynamic Modeling for Arbitrary Motions," *AIAA Journal*, Vol. 17, No. 4, 1979, pp. 365–374.
- ¹³Beddoes, T. S., "Practical Computation of Unsteady Lift," *Vertica*, Vol. 8, No. 1, 1984, pp. 55–71.
- ¹⁴Leishman, J. G., and Nguyen, K. Q., "A State-Space Representation of Unsteady Aerodynamic Behavior," *AIAA Journal*, Vol. 28, No. 5, 1990, pp. 836–845.
- ¹⁵Lomax, H., "Indicial Aerodynamics," *AGARD Manual on Aeroelasticity*, Oct. 1968, Chap. 6.
- ¹⁶Tobak, M., "On the Use of the Indicial Function Concept in the Analysis of Unsteady Motions of Wings and Wing-Tail Combinations," NACA Rept. 1188, Aug. 1954.
- ¹⁷Wagner, H., "Über die Entstehung des Dynamischen Auftriebes von Tragflügeln," *Zeitschrift für Angewandte Mathematik und Mechanik*, Vol. 5, No. 1, 1925, pp. 17–35.
- ¹⁸Küssner, H. G., "Zusammenfassender Bericht Unter den Instationären Auftreib von Flügeln," *Luftfahrtforschung*, Vol. 13, No. 20, 1936, pp. 410–424.
- ¹⁹von Kármán, T., and Sears, W. R., "Airfoil Theory for Non-Uniform Motion," *Journal of the Aeronautical Sciences*, Vol. 5, No. 10, 1938, pp. 379–390.
- ²⁰Sears, W. R., "Some Aspects of Non-Stationary Airfoil Theory and Its Practical Application," *Journal of the Aeronautical Sciences*, Vol. 8, No. 3, 1941, pp. 104–108.
- ²¹Bisplinghoff, R. L., Ashley, H., and Halfman, R. L., *Aeroelasticity*, Addison-Wesley, Reading, MA, 1955.
- ²²Leishman, J. G., "Indicial Lift Approximations for Two-Dimensional Subsonic Flow as Obtained from Oscillatory Measurements," *Journal of Aircraft*, Vol. 30, No. 3, 1993, pp. 340–351.
- ²³Leishman, J. G., "Subsonic Unsteady Aerodynamics Caused by Gusts Using the Indicial Method," *Journal of Aircraft*, Vol. 33, No. 5, 1996, pp. 869–879.
- ²⁴Miles, J. W., "The Aerodynamic Force on an Airfoil in a Moving Gust," *Journal of the Aeronautical Sciences*, Vol. 23, Nov. 1956, pp. 1044–1050.
- ²⁵Drischler, J. A., and Diederich, F. W., "Lift and Moment Responses to Penetration of Sharp-Edged Traveling Gusts, with Application to Penetration of Weak Blast Waves," NACA TN 3956, May 1957.
- ²⁶Lomax, H., "Lift Developed on Unrestrained Rectangular Wings Entering Gusts at Subsonic and Supersonic Speeds," NACA TN 2925, April 1953.
- ²⁷Heaslet, M. A., and Spreiter, J. R., "Reciprocity Relations in Aerodynamics," NACA Rept. 1119, Feb. 1952.
- ²⁸von Kármán, T., "Supersonic Aerodynamics—Principles and Applications," *Journal of the Aeronautical Sciences*, Vol. 14, No. 6, 1947, pp. 373–409.
- ²⁹Flax, A. H., "Relations Between the Characteristics of a Wing and its Reverse in Supersonic Flow," *Journal of the Aeronautical Sciences*, Vol. 16, No. 8, 1949, pp. 496–504.
- ³⁰Flax, A. H., "General Reverse Flow and Variational Theorems in Lifting-Surface Theory," *Journal of the Aeronautical Sciences*, Vol. 19, No. 6, 1952, pp. 361–374.
- ³¹Flax, A. H., "Reverse Flow and Variational Theorems for Lifting Surfaces in Nonstationary Compressible Flow," *Journal of the Aeronautical Sciences*, Vol. 20, No. 2, 1953, pp. 120–126.
- ³²Munk, M. M., "The Reversal Theorem of Linearized Supersonic Airfoil Theory," *Journal of Applied Physics*, Vol. 21, No. 2, 1950, pp. 159–161.
- ³³Brown, C. E., "The Reversibility Theorem for Thin Airfoils in Subsonic and Supersonic Flow," NACA TN 1944, Sept. 1949.
- ³⁴Jones, R. T., "The Minimum Drag of Thin Wings in Frictionless Flow," *Journal of the Aeronautical Sciences*, Vol. 18, No. 2, 1951, pp. 75–81.
- ³⁵Ursel, F., and Ward, G. N., "On Some General Theorems in the Linearized Theory of Compressible Flow," *Quarterly Journal of Mechanics and Applied Mathematics*, Vol. 3, Pt. 3, 1950, pp. 75–81.
- ³⁶Hariharan, N., and Leishman, J. G., "Unsteady Aerodynamics of a Flapped Airfoil in Subsonic Flow by Indicial Concepts," *Journal of Aircraft*, Vol. 33, No. 5, 1996, pp. 855–868.
- ³⁷Ffowles-Williams, J. E., and Hawkins, D. L., "Sound Generation by Turbulence and Surfaces in Arbitrary Motion," *Philosophical Transactions of the Royal Society of London, Series A: Mathematical and Physical Sciences*, Vol. 264, May 1969, pp. 321–342.
- ³⁸Lomax, H., Heaslet, M. A., Fuller, F. B., and Sluder, L., "Two and Three Dimensional Unsteady Lift Problems in High Speed Flight," NACA Rept. 1077, 1952.
- ³⁹McCroskey, W. J., and Goorjian, P. M., "Interactions of Airfoils with Gusts and Concentrated Vortices in Unsteady Transonic Flow," AIAA Paper 83-1691, July 1983.
- ⁴⁰Parameswaran, V., "Concepts for the Reduction of Blade Vortex Interaction Noise and the Use of CFD to Determine Indicial and Gust Responses of an Airfoil in Compressible Flow," Univ. of Maryland, Dept. of Aerospace Engineering, College Park, MD, Aug. 1995.
- ⁴¹Singh, R., and Baeder, J. D., "The Direct Calculation of Indicial Lift Response of a Wing Using Computational Fluid Dynamics," *Proceedings of the AIAA Applied Aerodynamics Conference* (New Orleans, LA), AIAA, Reston, VA, 1996, pp. 1041–1050.
- ⁴²Mazelsky, B., "Determination of Indicial Lift and Moment of a Two-Dimensional Pitching Airfoil at Subsonic Mach Numbers from Oscillatory Coefficients with Numerical Calculations for a Mach Number of 0.7," NACA TN 2613, Feb. 1952.
- ⁴³Mazelsky, B., and Drischler, J. A., "Numerical Determination of Indicial Lift and Moment Functions of a Two-Dimensional Sinking and Pitching Airfoil at Mach Numbers 0.5 and 0.6," NACA TN 2739, July 1952.
- ⁴⁴Srinivasan, G. R., and McCroskey, W. J., "Numerical Simulations of Unsteady Airfoil Interactions," *Vertica*, Vol. 11, No. 1/2, 1987, pp. 3–28.